PROCEEDINGS, Eighteenth Workshop on Geothermal Reservoir Engineering
Stanford University, Stanford, California, January 26-28, 1993
SGP-TR-145

# CORRELATING QUARTZ DISSOLUTION KINETICS IN PURE WATER FROM 25° TO 625°C

Jefferson W. Tester, W. Gabriel Worley, Bruce A. Robinson,
Charles O. Grigsby, Jeffrey L. Feerer

Massachusetts Institute of Technology
Chemical Engineering Department and Energy Laboratory
Cambridge, MA 02139

## BACKGROUND AND MOTIVATION

During the past 50 years, quartz dissolution kinetics and solubility measurements have been the subject of numerous investigations. Researchers have been motivated either because of their interest in understanding important natural geologic processes in the earth or because of a need to quantify dissolution rates for chemical processes above ground or for geothermal heat extraction underground. Our motivation for carrying out experimental studies of quartz dissolution for the last 15 years was driven by engineering issues related to mineral transport in circulating hot dry rock (HDR) geothermal systems (Armstead and Tester, 1987; Grigsby *et al.*, 1989; Charles *et al.*, 1979; Tester *et al.*, 1977). Of critical importance to HDR is the characterization of the rate of dissolution of host reservoir rock as a function of temperature, pressure and liquid phase composition. In general, quartz is a major mineral component in HDR reservoirs in low permeability crystalline rock. Furthermore, quartz is highly reactive relative to other constituent minerals in near neutral (non-acidic/non-basic) aqueous environments at temperatures of interest to HDR geothermal energy extraction (150° to 300°C). Because of these two reasons, we were motivated to understand the quantitative aspects of quartz dissolution in pure water.

More specifically, the analysis and modeling of data from HDR field tests at the Fenton Hill site in New Mexico require that dissolution kinetics be fully characterized in order to predict reservoir performances as well as to size the active reservoir on a volumetric or areal heat sweep efficiency basis (Grigsby and Tester, 1989). Because HDR systems have small circulating fluid volumes and residence times relative to natural hydrothermal systems, dynamic changes in dissolved silica concentration can be created by switching from a normal closed-loop mode of operating to an open-loop mode. In the closed-loop mode with a modest flow of make-up water, silica concentrations approach saturation because of recirculation effects. This permits the use of geothermometry to estimate reservoir temperatures (Fournier and Rowe, 1966). In the open-loop mode, however, fresh water with a low dissolved silica concentration can be flushed through the system. In this case the transport rate of silica into the reservoir fluid can be used as a chemical tracer to aid in estimating the size of the active heat transfer volume and area of the reservoir (Robinson *et al.*, 1988; Grigsby and Tester, 1989).

Given our motivation for examining quartz dissolution kinetics for HDR reservoir modeling needs, we started out in 1977 by carefully reviewing the available literature on this subject. We quickly realized that while a great amount of work had been done with quartz, results from one research group were rarely if ever compared with another group's data. Furthermore, there were only a few investigators who even attempted to correlate their data in a systematic manner. Over the last 15 years the situation has improved with respect to experimental procedures and equipment used along with a much improved appreciation for the importance of surface preparation and characterization. These factors have all contributed to enhancing the quality of the data. However, almost without exception, even recent investigators have not compared or correlated their rate data with others on a fully quantitative basis.

## THERMODYNAMICS AND KINETIC CONSIDERATIONS

In order to fully appreciate the manner in which dissolution rate data are correlated, several basic thermodynamic and kinetic issues germane to the quartz-water system are worthy of attention. Quartz dissolves congruently via a global hydrolysis pathway to form silicic acid ($Si(OH)_4$) (Iler, 1955, 1979).

$$SiO_{2(s)} + 2H_2O_{(aq)} \rightleftarrows Si(OH)_{4\,(aq)} \qquad (1)$$

Reaction (1) is reversible in the sense that both dissolution ($\rightarrow$) and precipitation ($\leftarrow$) pathways can occur simultaneously. At saturation, these rates are equivalent and the net rate of reaction is zero with dissolved silica values at levels corresponding to the solubility of quartz in water at a particular temperature, pressure, pH, etc. Studies reported in this paper deal specifically with dissolution measurements conducted in initially distilled and/or deionized water. Under these conditions and assuming that reactor wall materials are chemically inert, one would expect only temperature and, to a lesser extent, pressure to influence rates of dissolution.

Some investigators have employed the concepts of transition state theory to justify the form of a global rate expression for quartz dissolution (Rimstidt and Barnes, 1980; Brady and Walther, 1990; Dove and Crerar, 1990). While these approaches represent noteworthy extensions of transition state theory to heterogeneous (solid-liquid) geochemical kinetic systems, they do not identify rate-controlling elementary reaction steps at a molecular level. A recent treatment by Casey *et al.* (1990) using *ab initio* molecular orbital calculations provides a more realistic representation of possible transition state activated complexes. However, without direct evidence of activated complex structure in this heterogeneous system, a heuristic empirical approach is justified and can be useful in correlating dissolution rate data over a wide temperature range.

Although it is difficult to attribute original authorship to this idea, papers in the mid-1950's began to report a phenomenological rate equation based on de Donder and Nernst-like concepts (see for example, O'Connor and Greenberg, 1958; Iler, 1955). In this treatment, one postulates that reaction (1) is fully reversible; and that at saturation, the rate of dissolution equals the rate of precipitation. At conditions of undersaturation where the bulk concentration of silica in solution is below its solubility, the forward direction dissolution rate is assumed to occur at the same rate that it does at saturation while the precipitation rate decreases in direct proportion to the bulk silica concentration. In simple equation form this is equivalent to saying that the *net* rate of dissolution ($R_{diss}$) in mol/m$^2$ s is given at a particular temperature and pressure by the following expression

$$R_{diss} = \frac{-1}{V}\frac{dN_{SiO_2}}{dt} = k_d a^* (C^{sat}_{SiO_2} - C_{SiO_2}) \qquad (2)$$

and by defining $k^*_d \equiv k_d C^{sat}_{SiO_2}$,

$$R_{diss} = k^*_d a^* (1 - C_{SiO_2}/C^{sat}_{SiO_2}) \qquad (3)$$

where

$a^*$ = active quartz surface area per unit of fluid volume (m$^2$/m$^3$)

$k_d$ = empirical first-order dissolution rate constant (m/s)

$k^*_d \equiv k_d C^{sat}_{SiO_2}$ = empirical zero-order dissolution rate constant (mol/m$^2$ s)

$C_{SiO_2}$ = bulk silica concentration (mol/m$^3$)

$C^{sat}_{SiO_2}$ = saturated silica concentration or solubility (mol/m$^3$)

$V$ = solution or fluid volume (m$^3$)

$N_{SiO_2}$ = moles of silica dissolving from quartz (mol)

$t$ = time (s)

The term $(1 - C_{SiO_2}/C^{sat}_{SiO_2})$ can be viewed as the degree of undersaturation. One can see that $R_{diss}$ has a linear or first-order dependence on concentration, and at saturation $R_{diss}$ goes to zero. At the opposite extreme, $R_{diss}$ is maximized when $C_{SiO_2} = 0$. This condition is referred to as "free-dissolution" and is analogous to evaporation of a solid or liquid into a perfect vacuum.

In essence, this phenomenological approach assumes that the forward dissolution process in Reaction (1) occurs at a constant rate, independent of the composition of the surrounding bulk solution. Thus,

$$r_{diss} = r^{max}_{diss} = k_d a^* C^{sat}_{SiO_2} \qquad (4)$$

This forward rate is equal to the maximum, reverse precipitation rate at saturation. Consequently, the net rate $r^{max}_{diss} = k_d a^* C^{sat}_{SiO_2} = 0$ at saturation or

$$r^{max}_{diss} = r^{max}_{pptn} = k_p a^* C^{sat}_{SiO_2} \qquad (5)$$

and $k_d = k_p$. At finite undersaturations, $C_{SiO_2} < C^{sat}_{SiO_2}$ and $r_{pptn}$ is reduced in proportion to the bulk silica concentration:

$$r_{pptn} = k_p a^* C_{SiO_2} = k_d a^* C_{SiO_2} \qquad (6)$$

Therefore, Eqn. (2) can be developed by subtracting Eqn. (6) from Eqn. (5). We want to emphasize that either derivation of Eqn. (2) does not require a molecular-level, elementary reaction description of the quartz dissolution mechanism.

The a* term in Eqns. (2)-(6) underscores the importance of knowing the active dissolving surface area. Many investigators report that the BET-derived surface area from nitrogen or argon gas adsorption is the correct surface area to use -- but they do not provide molecular-based reasoning to justify that claim. At the opposite extreme, a nominal value of the surface area based on the bulk geometric characteristics of the quartz sample can be used depending on whether it is a slab, disc, cylinder or crushed into a quasi-spherical rough particle shape. White and Peterson (1990a, b) give an excellent review of surface area concerns as they apply to geochemical kinetics in natural systems undergoing weathering.

In principle, the forward dissolution rate should depend on the concentration of active ≡ Si-O-Si ≡ sites on the surface. As a first approach, we can assume that the dissolution rate varies linearly with the surface site concentration and that the concentration of active ≡ Si-O-Si ≡ sites scales directly with the *saturation* value of silica dissolved in the bulk aqueous phase. Given these assumptions, classical phase equilibrium considerations enter the picture. The $C^{sat}_{SiO_2}$ term in Eqn. (2) expresses this effect quantitatively, with the forward dissolution rate of Reaction (1) given by Eqn. (4).

Effectively, because we measure the net dissolution rate ($R_{diss}$) and the bulk silica concentration in solution $C_{SiO_2}$ and estimate a*, in order to extract a first-order rate constant for dissolution ($k_d$) we need to have an estimate of $C^{sat}_{SiO_2}$ as a function of temperature and pressure in the two-component, binary mixture of quartz ($SiO_2$) and water ($H_2O$).

Fournier and Potter (1982) provide an excellent correlation for quartz solubility. Figure 1 compares their solubility correlation at the vapor pressure of the solution and at 1000 bar with experimental data from several investigators (Kennedy, 1950; Crerar and Anderson, 1971; Hemley *et al.*, 1980; Morey and Hesselgesser , 1951; Siever, 1962). Data are given from 25°C to the critical point of pure water at 374°C on the saturation curve, while they extend to 600°C at 1000 bar.

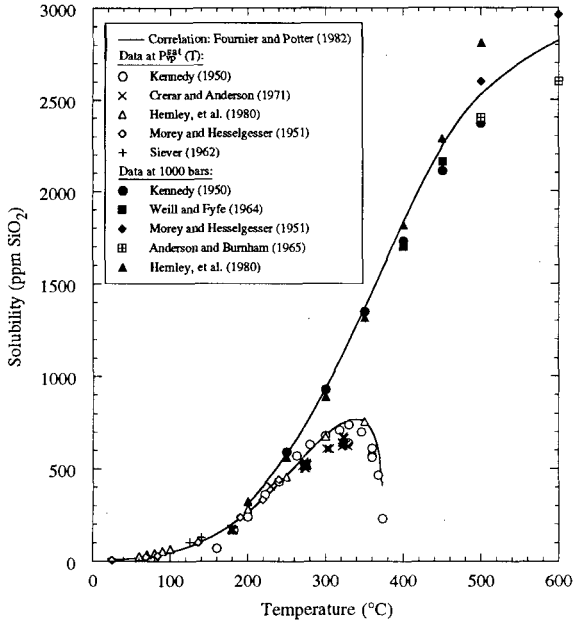


Figure 1. Solubility of quartz in pure water at the saturated solution vapor pressure and at 1000 bar

Figure 2 gives a semi-logarithmic plot of both the vapor pressure ($P^{sat}_{vp}$) of pure water and the solubility ($C^{sat}_{SiO_2}$) as a function of reciprocal absolute temperature. These so-called Gibbs-Helmholtz coordinates linearize the temperature dependence and provide an estimate of phase transition enthalpies from the slope of the lines -- $\Delta H$ (vaporization) from the vapor pressure line and $\Delta H$ (solution) from the solubility line. The highly non-linear behavior for solubility near the critical point is indicative of a change in the solvation characteristics of water on a molecular level.

The Fournier and Potter correlation for quartz solubility used in our data analysis is as follows:

$$\log_{10} C_m = A + B\,(\log_{10} v) + C(\log_{10} v)^2 \qquad (7)$$

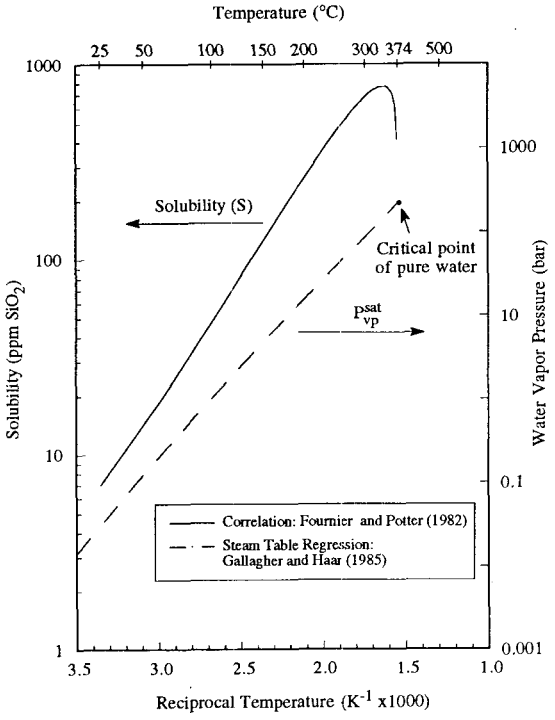


Figure 2. Vapor pressure of pure water and quartz solubility at the saturation vapor pressure from 25°C to the critical point (374°C, 221 bar) using Gibbs-Helmholtz coordinates to linearize temperature dependencies

where A, B, and C are empirical temperature-dependent constants that have been fit to data, $C_m$ is the molal silica concentration (moles $SiO_2$/1 kg of water), v is the specific volume of water (cc/g) and T is the temperature in Kelvins. The A, B, and C parameters are given by

$$A = 4.66206 + 0.0034063\,T + 2179.7\,T^{-1} - 1.1292 \times 10^6\,T^{-2} + 1.3543 \times 10^8\,T^{-3}$$

$$B = -0.0014180\,T - 806.97\,T^{-1}$$

$$C = 3.9465 \times 10^{-4}\,T$$

We can rewrite Eqn. (2) to express the solubility $C^{sat}_{SiO_2}$ in ppm (parts per million of $SiO_2$) as:

$$\log_{10} C^{sat}_{SiO_2} = \log_{10}(C_m \times MW) \times 10^3) = 4.7788 + \log_{10} C_m \qquad (8)$$

where MW = molecular weight of $SiO_2$ = 60.084.

Equations (2) and (3) thus represent an empirical global model for quartz dissolution that can be used to correlate data. If we can show that it is applicable over a wide range of conditions, then one not only gets a useful function for correlating data but its simple mathematical form can be easily incorporated into dynamic reservoir simulation models.

## SPECIFIC OBJECTIVES AND APPROACH

Given the motivating factors cited in the previous section, our objectives in preparing this paper were twofold: first to describe our experimental procedures for preparing and characterizing quartz surfaces and carrying out kinetic measurements of dissolution rates from 25° to 255°C and second to compare and correlate our results with kinetic data reported by other investigators in developing a general empirical correlation for intrinsic dissolution kinetics.

Our approach to achieving these objectives consisted of the following key steps:

(1) designing and utilizing five different experimental systems for measuring dissolution rates

(2) developing consistent procedures for sample preparation and composition measurements so that reproducible kinetic data could be obtained

(3) analyzing all existing published kinetic data on quartz dissolution in pure water to determine their suitability for quantitative correlations

(4) conducting dissolution experiments from 25° to 255°C

(5) developing an empirically-based model to correlate our data with those collected in other laboratories

## EXPERIMENTAL EQUIPMENT AND PROCEDURES EQUIPMENT

**Equipment.** Five different apparatus were used in this study to obtain dissolution kinetic data. For purposes of identification we have labeled them:

(1) *Batch Bottle*
(2) *Packed Bed*
(3) *Rocking Autoclave*
(4) *Stirred Autoclave*
(5) *Spinning Basket*

The *Batch Bottle* system is simply a sealed polyethylene bottle (125 ml) that contains the quartz sample in water. This apparatus was used only for measurements in the temperature range of 23° to 50°C. Solution samples were removed periodically for analysis and temperatures were maintained in a constant-temperature water bath to ± 1°C. Typically, experiments at these temperatures were conducted from 4 to 18 months.

The *Packed Bed* system (Grigsby, 1989) used a vertical cylindrical teflon-lined stainless steel reactor (4.13 cm diameter and 15.24 cm long). The reactor contained a 13 cm high packed bed of quartz particles suspended vertically on teflon-coated, stainless steel filter holder. All wetted parts in the system were either polyethylene or Teflon. Water was pumped into the bottom of the bed which contained 288.0 g of quartz sand with a void fraction of 39.2%. Liquid samples were taken from the effluent in the top of the reactor where pH was also measured. All experiments in the *Packed Bed* reactor were conducted at 25°C. Tracer tests indicated that non-ideal flow due to dispersion in the packed bed was insignificant. Ideal plug flow behavior with a uniform fluid velocity in the bed was closely approximated, thus the system could be treated as a plug flow reactor (PFR) for purposes of data analysis.

The *Rocking Autoclave* system (Robinson, 1982) consisted of a small, closed reactor bomb agitated using a reclining arm to raise and lower the vessel which was kept isothermal using band heaters and an Athena differential temperature controller. Alternatively, the bomb was placed in an oven and whole system was rocked to achieve adequate mixing between the solid quartz particles and fluid phase. The bombs used in this study were constructed of titanium with a teflon O-ring used to seal the cover. Their inside dimensions were 2.29 cm diameter with a length of 5.23 cm -- providing a working volume of about 21.5 $cm^3$. The *Rocking Autoclave* apparatus was used for measurements from 200 to 250°C. Separate runs were carried out over a range of exposure times to obtain rate information as only the final concentration of the solution was determined after the dissolution reaction had been quenched using liquid nitrogen or cold water to cool the bomb.

The *Stirred Autoclave* experimental apparatus (Robinson, 1982) was used to perform batch quartz dissolution experiments in the temperature range from 180° to 255°C. The reactor vessel was a Pressure Products Industries, 316 stainless steel autoclave, with a total usable volume of approximately 1 L. A variable speed D.C. motor drives a rotating magnet to which a six-bladed agitation propeller/shaft assembly is attached. The rotation speed was adjusted from approximately 200-900 rpm to ensure good mixing. Liquid samples were extracted from the autoclave through a sampling valve connected to a small diameter stainless steel tube which was immersed in a cold water bath to cool the liquid sample well below its boiling point. Constant temperature to ± 1°C was maintained using an external electrical resistance heating jacket controlled by an Athena temperature controller, which received its temperature signal from a thermocouple placed in the immersed thermocouple well.

To perform an experiment, a sample of crushed quartz of known weight and size fraction was charged through the top of the reaction vessel. A known amount of distilled, deionized water (usually 500 mL) was then added and the system closed to begin heatup. The water was preheated to cut down on the time required for the system to reach the desired temperature. The reactor and contents were allowed to heat up without turning on the stirrer; this procedure minimized the dissolution rate during the heatup period. Once the desired temperature was reached, samples were taken at regular intervals as follows: the stirrer, which was operating constantly

during the experiment, was shut off for about one minute before a sample was taken to allow the solid particles to settle to the bottom of the autoclave. Then approximately 4 mL of liquid were expelled to displace the stagnant fluid in the sampling tube. Then roughly 3 mL of sample were taken and the stirrer turned back on. At the end of an experiment, the stirrer and controller were turned off and the system allowed to cool just below the boiling point of water. This temperature is high enough that none of the dissolved silica would reprecipitate on the quartz particles upon cooling. The entire contents were then drained and the quartz particles rinsed thoroughly before being used in the next experiment.

The final reactor system used in this study was a *Spinning Basket* flow-through design, developed to improve reaction conditions by reducing the interparticle abrasion that occurs in the other two autoclave systems. Quartz particles were held in an annular fixed bed using a rigid wire screen basket which is rotated within an autoclave vessel to maintain good fluid contact and high mass transfer rates, and to virtually eliminate abrasion effects common to fluidized bed or actively stirred or rocked reactor systems. In the *Spinning Basket* system all wetted parts at dissolution conditions were constructed of CP (commercially pure) titanium.

The Ti *Spinning Basket* reactor system and ancillary equipment are schematically shown in Fig. 3. An Autoclave Engineers magnetic drive unit was modified to provide rotation of the Ti basket containing the quartz sample. A 20 L polypropylene feed tank was used to hold the distilled, deionized water that was fed continuously to the reactor to maintain well-mixed conditions for this open, flow-through design. A charge of approximately 600 g of prepared Ottawa sand was used for all experiments. The reactor has a liquid volume of approximately 1 L; thus a nominal surface area to fluid volume ratio of 19 $cm^2/cm^3$ could be maintained to permit operation over a wide range of

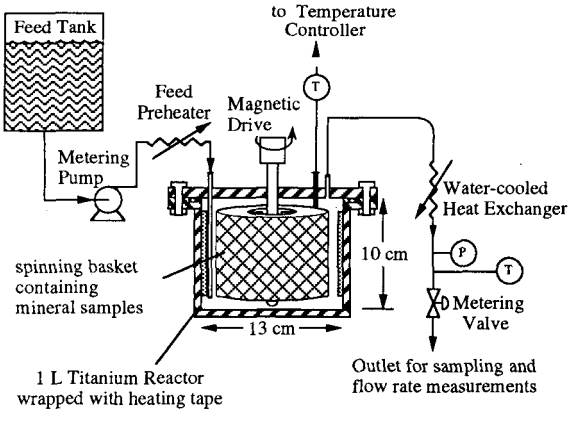


Figure 3. Schematic of the titanium spinning basket continuous flow stirred tank reactor (CSTR) system

temperatures and residence times ($\tau$). At 70°C, the feed water flow rate was 0.3 mL/min ($\tau$ = 3300 min) while at the maximum temperature studied of 150°C, the flow rate was 20 mL/min ($\tau$ = 50 min). Under these conditions we could maintain ideal back-mixed flow and still observe measurable dissolved $SiO_2$ concentrations in the product effluent stream from the reactor. The *Spinning Basket* reactor had a maximum operating pressure of 8 bar (116 psia) which limited the temperature to about 150°C for dissolution runs where the vapor pressure of water is 4.75 bar (68.9 psia). The system has now been upgraded to operate at 240°C and 40 bar (600 psia) for experiments currently underway. A Na-fluorescein dye tracer study performed on this reactor indicated that, to within experimental accuracy, ideal continuous stirred tank reactor (CSTR) flow conditions existed with a residence time distribution (RTD) given by:

$$f(t) = 1 - \exp[-t/\tau] \qquad (9)$$

where f(t) maps out the time dependence of the tracer concentration in the product stream in response to a unit concentration step change in the feed and $\tau$ is the mean reactor residence time ($V_R/\dot{q}$; $V_R$ = reactor volume and $\dot{q}$ = volumetric flow rate).

Other equipment supporting the *Spinning Basket* reactor included an electrically heated preheater tube for the feed and a water-cooled heat exchanger for the product. Both of these employed CP titanium tubing. The reactor itself was wrapped in heating tape and insulated to maintain isothermal conditions. Following the cool-down section when the product stream reached about 30°C or less, titanium tubing and 316 stainless steel fittings were used.

**Sample Preparation.** In our experiments two types of quartz were used: crushed, clear, Hot Springs, Arkansas, quartz crystals and Ottawa sand. For both samples cleaning and washing steps were used to ensure well-defined uniform surfaces. Crushing and other types of mechanical deformation can create a disturbed surface layer which, if not taken into account properly, can falsify the data resulting from a quartz dissolution experiment. Other experimenters (Van Lier *et al.*, 1960; Rimstidt and Barnes, 1980) observed initial rapid rates of dissolution as a result of a disturbed layer. Rimstidt and Barnes (1980) hypothesized that these high rates were a result of a thin layer of amorphous silica and used their early time data to obtain an estimate for the dissolution rate of amorphous silica. An equally plausible mechanism would be that the initially high rate is due to a larger a* term in Eqn. (2) that is caused by very small particles (fines) that were created by mechanical deformation during crushing or are present from purely natural causes.

Scanning electron microscope (SEM) photographs were used in the present study to verify the existence of the damaged layer. Figure 4a is a SEM photograph of an unwashed particle of quartz taken using an ISI Model DS-130 scanning electron


(a) Untreated crushed quartz.


(b) Reacted crushed quartz after several dissolution experiments above 150°C.

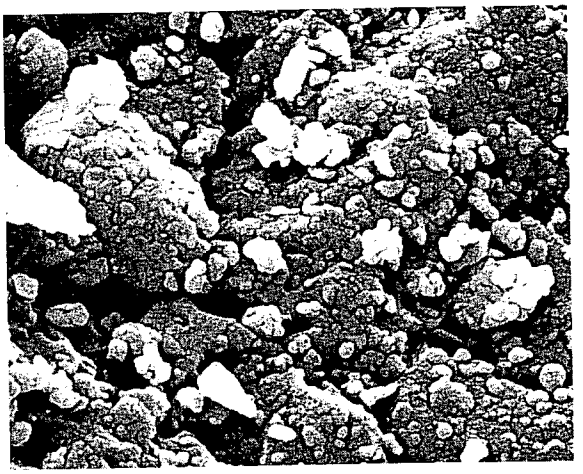


(c) Untreated Ottawa sand.

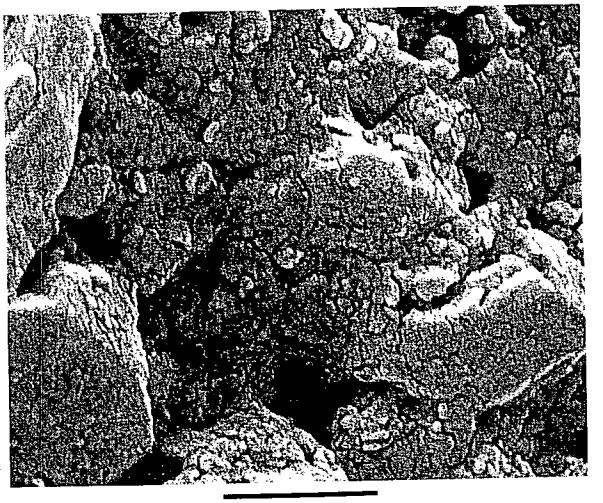


(d) Washed Ottawa sand.

Figure 4. Scanning Electron Microscope (SEM) photograph of typical crushed quartz and Ottawa sand before and after treatment to remove fines.

microscope. Clearly, the damaged layer exists as a discontinuous collection of fines adhering to the surface of the particle. Even if the small fines were pure amorphous silica, obtaining an accurate value for the surface area is not feasible. Thus, extracting meaningful amorphous silica kinetic data from a quartz dissolution experiment using the initial rate data is problematic. Furthermore, some of the fines may have small enough radii of curvature (of the order of 1 μm or less) that surface energy effects could significantly raise their equilibrium solubility in water via a Gibbs-Kelvin-Thompson effect.

The initial rapid dissolution of these small particles suggests an effective method to get around the problem of fines adhering to the quartz surface. If the quartz particles are brought to a high temperature in water (200°C or greater) for several hours, then the fines will dissolve preferentially until they have been totally eliminated. In practice, the method used in this study was simply to reuse the same quartz particles in each experiment. The first experiment using freshly prepared quartz particles always exhibited a rapid initial rate of dissolution. Subsequent experiments did not, suggesting that the small fines had been dissolved completely in the first experiment. Figure 4b is a SEM photograph of a typical crushed quartz particle after several runs at high temperature (> 200°C). The fines have been virtually eliminated, ensuring that the subsequent dissolution experiments are those of the large quartz particles with no interference from the small fines.

Van Lier (1960) showed that treatment with HF will dissolve the fines very rapidly. However, since HF chemically interacts with quartz to accelerate dissolution, an elaborate washing procedure is necessary to ensure that none of the HF is left in the microfractures of the quartz particles. The procedure suggested in the present study is much easier to carry out experimentally, and avoids the problem of HF adsorption into the microfractures.

One piece of empirical evidence obtained from our *Stirred Autoclave* experiments (180° to 255°C) suggests that the small fines are responsible for the rapid initial rate of dissolution. During the 1 to 2 hours required to heat the reactor up to temperature, the amount of dissolution predicted from the rate expression of Eqn. (2) is so small that the initial concentration of dissolved silica (the concentration after the system has reached its ultimate temperature) should still be approximately 0 ppm. Experimentally, this calculation is borne out in the runs performed using annealed quartz, but the first experiment using unwashed quartz shows that the concentration reaches at least 40 ppm during the heatup period. Presumably this initial higher concentration is due to rapid dissolution of the small fines. If Figure 4a is taken as a typical example of the size and quantity of the fines, then it can be calculated that complete dissolution of these small particles during heatup would result in an initial concentration within a factor of 2 of the observed 40 ppm. Given the limited accuracy of such a calculation, the fact that it results in a concentration in the neighborhood of the observed result suggests that rapid dissolution of the small fines is a reasonable explanation of the initial dissolution rate behavior.

Crushed quartz was used for all dissolution experiments conducted in the *Rocking Autoclave* and *Stirred Autoclave*, batch reactor systems. Quartz crystals were crushed, washed and sieved to obtain a desired size range. For the *Rocking Autoclave* experiments, a 53 to 1000 μm size distribution was used; while for the *Stirred Autoclave* runs, a narrower size distribution of 53 to 149 μm was used. These represent overall particle size ranges while actual ranges used in individual experiments were considerably smaller.

Ottawa sand was used for all dissolution experiments carried out in the *Packed Bed* (PFR), *Batch Bottle*, and *Spinning Basket* (CSTR) reactor systems. Samples of Ottawa sand were prepared slightly differently depending on the reactor used. The preparation procedure was as follows:

1. Wash the *as received* 20 to 28 mesh (595 to 841 μm) sand particles for 10 minutes in concentrated nitric acid to remove iron.
2. Tumble for three weeks with continued, periodic fresh water washes (500 mesh silicon carbide grit was used for the sand particles used in the *Packed Bed* reactor runs).
3. Rinse with water.
4. Wash with water for three weeks with fresh water added periodically.
5. Dry at 100°C (an ethanol wash was used before drying for the sand particles used in the Packed Bed reactor runs).

**Analytical Methods.** Three primary methods -- molybdate yellow and blue spectrophotometric and inductively coupled plasma (ICP) emission spectroscopy -- and one secondary method -- atomic absorption (AA) spectroscopy -- were used to determine dissolved silica concentrations. The molybdate yellow method was used for $SiO_2$ concentrations in the 1 to 400 ppm range while the molybdate blue and ICP methods were used in the 0.02 to 2.0 ppm range. AA was used periodically to cross-check the molybdate techniques to ensure that silica polymerization was not significantly affecting the determination of dissolved $SiO_2$.

The color reagent for the molybdate yellow method was prepared by mixing 50 ml of 1.0 N sulfuric acid with 20 ml of a premixed 10 wt% ammonium molybdate solution and diluting to 500 ml with deionized water. The ammonium molybdate solution was prepared by dissolving an appropriate amount of reagent grade ammonium molybdate pellets in deionized water to obtain a 10% by wt. solution. The concentrated sulfuric acid used to prepare the 1.0 N $H_2SO_4$ solution was also of reagent grade purity.

Fresh quantities of yellow color reagent were prepared every day during an experimental run since it was observed that the transmittance of light in the reagent declines noticeably after a few days. To perform an analysis, 1.0 ml of sample was pipetted and diluted to 50.0 ml in a volumetric flask. Transmittance readings at 6, 9, and 12 minutes after the start of the reaction were taken at a wavelength of 440 nm and 0.098 μm slit width using a Beckman DU-2 spectrophotometer. For almost all samples, two agreeing transmittance readings (to the third decimal place) were obtained in these three readings.

The transmittance readings were converted to concentrations assuming Beer's law was followed. To verify the Beer's law assumption, a 1000 ppm sodium silicate standard was diluted quantitatively to 50, 100, and 200 ppm and the absorbance was found to vary linearly with concentration over this range.

The molybdate blue method utilized absorbance at 815 nm measured on a Schimadzu UV-160U spectophotometer following a ASTM standard technique #D859. Calibration was carried out using quantitative dilutions of a silicon AA standard solution (1010 ppm Si in 2% NaOH) to establish a linear Beer's law region from 0.1 to 2.0 ppm $SiO_2$. Both molybdate methods are accurate to about ± 3% (with slightly higher errors near the lower detection limit).

ICP measurements were carried out at 251.61 nm for $SiO_2$ using a Perkin-Elmer model 5500 ICP emission spectrograph for the runs carried out in the *Packed Bed* (PFR) reactor system at 25°C. ICP analyses were performed by D. Counce of Los Alamos National Laboratory. Although a detection level of about 1 ppb is possible for silica, lower limits of 20 ppb (0.02 ppm) were reported for our measurements.

## CORRELATION OF EXPERIMENTAL DISSOLUTION KINETICS DATA

Dissolution experiments were performed using the five different reactor systems described in the preceding section. Operating conditions for each system were tabulated in Table 1. Also included are run conditions, reactor designs and mineral descriptions for seven studies of quartz dissolution from other laboratories that were selected for correlation and comparison with our data. As can be seen from Table 1, values for nominal surface area, BET area, and surface area per unit fluid volume are given. The nominal areas are based on average particle sizes using an effective spherical radius (<r>) and the density of quartz (r)

$$\text{Nominal area} = \frac{4\pi(<r>)^2}{(4\pi/3)(<r>)^3\rho} = \frac{3}{<r>\rho} \qquad (10)$$

BET areas reported in our studies used $N_2$/He adsorption and standard methods. Values for other investigators were cited if available in their published results.

Dissolution rate data as a function of temperature for experiments carried out in this investigation are given in Table 2. Both $k_d^*$ and $C_{SiO_2}^{sat}$ values are provided so that either $k_d = k_d^* / C_{SiO_2}^{sat}$ or $k_d^*$ values can be correlated to temperature. The method used to estimate $k_d$ or $k_d^*$ depends on experimental conditions. Batch experiments in the *Rocking Autoclave*, *Stirred Autoclave*, and *Batch Bottle* systems were analyzed using a time integration of Eqn. (2) that accounted for any volume changes that occured due to periodic sampling (see Robinson, 1982 for details). Continuous flow, open system experiments in the *Packed Bed* (PFR) and *Spinning Basket* (CSTR) system utilized conventional chemical engineering methods for reactor analysis (see Grigsby, 1989 for details).

Table 1. Experimental reaction conditions, reactor designs, and mineral descriptions

| Investigator | Reactor Type[1] | Reactor System Wetted Material | Temp Range (°C) | Mineral Type[2] | Particle Size | Specific Surface Area ($cm^2/g$) | | nominal area[3] / fluid volume ($cm^2/cm^3$) |
|---|---|---|---|---|---|---|---|---|
| | | | | | | nominal | BET | |
| *Present Study:* | Rocking Autoclave (B) | Titanium | 200-250 | Crushed AK | 53-1000 μm | 12-352 | - | 1.6 |
| | Stirred Autoclave (B) | 316 SS | 184-255 | Crushed AK | 53-149 μm | 126-212 | - | 7-44 |
| | Packed Bed (PFR) | Teflon-lined SS | 25 | Ottawa Sand | 595-841 μm | 32 | 766-903 | 108 |
| | Batch Bottle (B) | Polyethylene | 23-50 | Ottawa Sand | 595-841 μm | 32 | 766-903 | 3-48 |
| | Spinning Basket (CSTR) | CP Titanium | 70-150 | Ottawa Sand | 595-841 μm | 32 | 766-903 | 19 |
| Brady and Walther (1990) | Floating Bottle (B) | "Plastic" | 25 | Crushed AK | 74-149 μm | 210 | 1110 | 7-32 |
| Dove and Crerar (1990) | Mixed Flow (CSTR) | CP Titanium | 200-300 | Crushed AK | 150-250 μm | 116 | 230 | 0.76 |
| Kitahara (1960) | Autoclave (B) | Silver-lined steel | 400-480 | Slab | 5x10x15 mm | - | - | 0.16 |
| Rimstidt and Barnes (1980) | Rocking Autoclave (B) | --- | 65-305 | Sand (Corning) | 100-1000 μm | 54 | 920 | 67-2600 |
| Siebert, et al. (1963) | Spinning Disc (B) | Stainless Steel | 248-332 | Disc (0001) | 64.8 mm diam | - | - | 0.033 |
| van Lier, et al. (1960) | Rotating Tube (B) | Platinum | 70-90 | Crushed BZ | 5-10 mm | 3140 | 3600 | 290 |
| Weill and Fyfe (1964) | Autoclave (B) | Inconel | 400-625 | Slab AK (0001) | - | - | - | 0.1-0.2 |

[1] B = batch - closed system
CSTR = *continuous flow stirred tank reactor*
PFR = plug flow reactor

[2] AK = Hot Springs, Arkansas Quartz
BZ = Brazilian Quartz

[3] a*(nominal basis) = nominal area/fluid volume ; 1 $cm^2/cm^3$ = 100 $m^2/m^3$

Table 2. Quartz nominal dissolution rate constant data from the present study and earlier investigations plotted in Figure 5

| Present Study | Temp (°C) | $\log_{10} k_d^{*}$ [1] (mol/m$^2$-s) | $C_{SiO_2}^{sat}$ [2] (ppm) | Earlier Studies | Temp (°C) | $\log_{10} k_d^{*}$ [1] (mol/m$^2$-s) | $C_{SiO_2}^{sat}$ [2] (ppm) |
|---|---|---|---|---|---|---|---|
| *Packed Bed* | ****25 | -11.00 | 7 | Brady and Walther (1990) | | | |
| | ****25 | -11.65 | 7 | *Floating Bottle* | ****25 | -11.19 | 7 |
| | | | | | ****25 | -11.73 | 7 |
| *Batch Bottle* | ****23 | -12.58 | 7 | Van Lier, et al. (1960) | | | |
| | ****23 | -12.61 | 7 | *Rotating Tube* | 70 | -12.16 | 24 |
| | ****23 | -12.45 | 7 | | 80 | -11.46 | 30 |
| | ****23 | -12.55 | 7 | | 90 | -11.16 | 38 |
| | 23 | -13.42 | 7 | | ***90 | -11.64 | 38 |
| | 23 | -13.27 | 7 | | ***90 | -11.02 | 38 |
| | 50 | -12.19 | 14 | | ***90 | -11.20 | 38 |
| | 50 | -12.20 | 14 | Rimstidt and Barnes (1980) | | | |
| | 50 | -12.21 | 14 | *Rocking Autoclave* | *65 | -10.60 | 21 |
| *Spinning Basket* | 70 | -11.34 | 24 | | **105 | -9.14 | 53 |
| | 100 | -10.19 | 48 | | *105 | -9.88 | 53 |
| | 100 | -10.22 | 48 | | 105 | -10.27 | 53 |
| | 100 | -10.19 | 48 | | **105 | -10.18 | 53 |
| | 100 | -10.44 | 48 | | 145 | -8.36 | 115 |
| | 125 | -9.27 | 79 | | **145 | -9.01 | 115 |
| | 125 | -9.19 | 79 | | 170 | -8.43 | 173 |
| | 125 | -9.07 | 79 | | **187 | -8.11 | 221 |
| | 125 | -9.16 | 79 | | *213 | -7.07 | 311 |
| | 125 | -9.17 | 79 | | 265 | -6.56 | 529 |
| | 125 | -9.53 | 79 | | 305 | -6.14 | 698 |
| | 125 | -9.63 | 79 | Dove and Crerar (1990) | | | |
| | 125 | -9.61 | 79 | *Mixed Flow (CSTR)* | 200 | -7.63 | 269 |
| | 125 | -9.81 | 79 | | 200 | -7.35 | 269 |
| | 125 | -9.58 | 79 | | 200 | -7.28 | 269 |
| | 150 | -8.39 | 125 | | 200 | -7.38 | 269 |
| | 150 | -8.46 | 125 | | 200 | -7.26 | 269 |
| | | | | | 201 | -7.43 | 272 |
| *Stirred Autoclave* | 184 | -7.84 | 212 | | 250 | -6.74 | 474 |
| | 184 | -7.98 | 212 | | 300 | -5.97 | 695 |
| | 184.5 | -8.20 | 213 | | 300 | -6.01 | 695 |
| | 202 | -7.31 | 270 | | 300 | -6.15 | 695 |
| | 202.5 | -7.43 | 272 | Siebert et al. (1963) | | | |
| | 203 | -7.24 | 274 | *Spinning Disc* | 248 | -6.11 | 476 |
| | 215 | -7.04 | 318 | | 250 | -5.99 | 486 |
| | 221 | -6.75 | 341 | | 269 | -5.85 | 579 |
| | 221 | -6.91 | 341 | | 291 | -5.54 | 688 |
| | 221 | -7.03 | 341 | | 315 | -5.16 | 793 |
| | 253 | -6.36 | 475 | | 332 | -4.96 | 843 |
| | 255 | -6.44 | 485 | Kitahara (1960) | | | |
| | | | | *Autoclave* | 400 | -4.46 | †360 |
| *Rocking Autoclave* | 200 | -7.04 | 264 | | 400 | -4.37 | †800 |
| | 200 | -7.20 | 264 | | 440 | -4.18 | †1840 |
| | 200 | -7.18 | 264 | | 440 | -4.37 | †1100 |
| | 250 | -6.66 | 463 | | 440 | -4.53 | †530 |
| | | | | | 480 | -4.43 | †750 |
| | | | | | 480 | -4.21 | †1580 |
| | | | | Weill and Fyfe (1964) | | | |
| | | | | *Autoclave* | 400 | -3.85 | 2015 |
| | | | | | 625 | -2.54 | 2896 |

1 $\log_{10} k_d^{*}$ were calculated using equation (3) and nominal values of a*

2 $C_{SiO_2}^{sat}$ were estimated using correlation by Fournier and Potter (1982) except values preceded by a †.

† Solubility values are based on actual measurements from Kitahara (1960).

Data points with asterisks were omitted from regression for the following reasons:

* ⇒ precipitation experiment
** ⇒ disturbed quartz surface
*** ⇒ experiments not designed to gain kinetic information
**** ⇒ outliers: quartz surfaces probably have not reached a steady state morphology

Figures 5 and 6 correlate the dissolution rate data from 25° to 625°C cited in Table 2 using nominal and BET-derived surface area estimates for the a* term in Eqn. (2). Both figures are in the form of Arrhenius ($\log_{10} k_d^*$ vs 1/T) plots. Data from the five reactor systems of our investigations are combined with the results of the seven previous research groups to arrive at linear-least squares correlations over the entire temperature range.

Empirical equations for $k_d^*$ based on the least-squares lines in Figs. 5 and 6 are given as:

$$k^*_{d,NA} = 475 \pm 356 \exp\left[-\frac{92.2 \pm 2.8}{RT}\right] \quad \text{(nominal area basis)} \qquad (11a)$$

$$k^*_{d,BET} = 597 \pm 1186 \exp\left[-\frac{101.3 \pm 6.6}{RT}\right] \quad \text{(BET area basis)} \qquad (11b)$$

where the error limits represent fits to a 95% confidence level and the units of $k^*_{d,NA}$ and $k^*_{d,BET}$ are mol/m$^2$ s, T is in Kelvins and R is in units of kJ/mol K. Overall, we estimate $\log_{10} k_d^*$ errors to be ± 0.64 using a nominal area basis and ± 0.98 using a BET area basis.

Although the scatter in the Fig. 5 data where $k_d^*$ is based on nominal area seems somewhat less than in Fig. 6 where $k_d^*$ is based on BET-derived areas, the apparent superior fit may be fortuitous. Nonetheless, both plots confirm the form of Eqn. (3) as a reliable empirical correlation which can be used with confidence to predict the rate of quartz dissolution in pure water over twelve-orders of magnitude of rate change from 25° to 625°C. This rather surprising result suggests that the global averaging effects of Eqns. (2) and (3) provide an accurate representation of dissolution kinetics in a traditional Arrhenius framework. Furthermore, the apparent activation energies of 92.2 ± 2.8 kJ/mol (nominal area basis) and 101.3 ± 6.6 kJ/mol (BET area basis) are reasonable in that they both agree with each other. For comparison, the estimated bond energy for breaking an Si-O bond is about 228 kJ/mole (Robie *et al.*, 1979), which suggests that the activated state to produce a free aqueous species of $SiO_2$ involves the formation of OH linkages to the dissolving $SiO_2$ species.

One would expect that the fundamental kinetic processes associated with dissolution would dominate the temperature dependence of Eqns. (2) and (3). These intrinsic kinetic effects are captured in the $k_d$ and $k_d^*$ global rate parameters. The a* term merely scales or normalizes one set of rate data to another and should not be as strongly temperature-dependent as $k_d$ or $k_d^*$. The observed similar activation energies for nominal- and BET-area normalizations and the similar quality of the correlations themselves shown in Figs. 5 and 6 support these assertions and further substantiate that the form used in Eqns. (2) and (3) is phenomenologically correct.

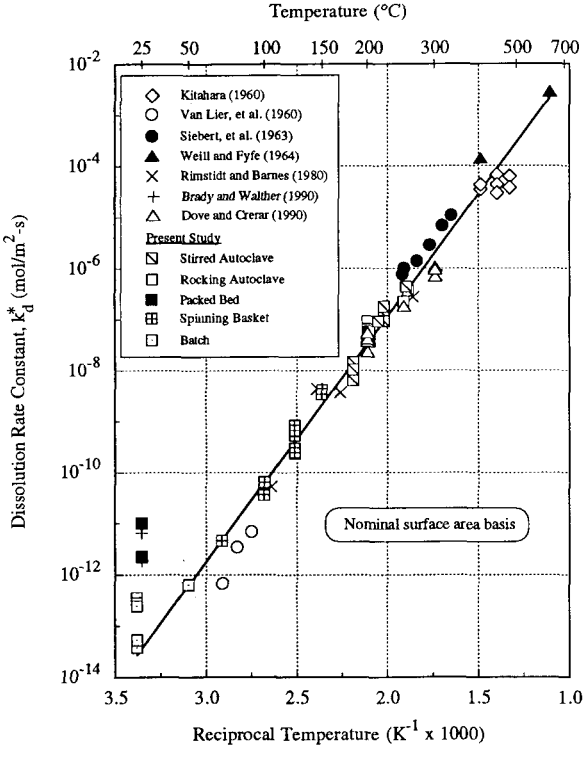


Figure 5. Quartz dissolution kinetics in pure water from 25° to 625°C using a nominal surface area basis and Arrhenius coordinates

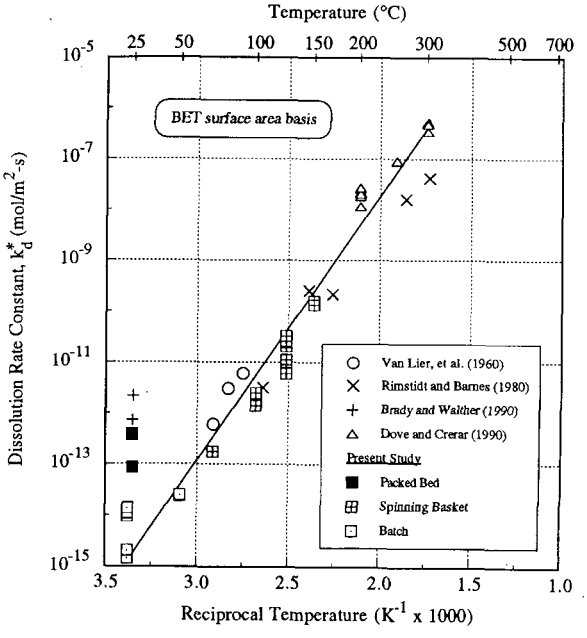


Figure 6. Quartz dissolution kinetics in pure water from 25° to 300°C using a BET-determined surface area basis and Arrhenius coordinates

There are several points that need to be made concerning the data given in Tables 1 and 2. First, not all values of $k_d^*$ available from previous investigators were plotted in Figs. 5 and 6. For example, as indicated in Table 2, several values given by Rimstidt and Barnes (1980) were omitted because a disturbed surface layer existed during their experiments. Also three data points reported by Van Lier *et al.* (1960) at 90°C were deleted because they came from experiments not designed to obtain kinetic information. Although several other investigators report quartz dissolution kinetics at pH's comparable to pure water conditions, they employed buffered solutions (Brady and Walther, 1990; Knauss and Wolery, 1988; Wollast and Chou, 1986). To avoid complications or ambiguities in interpretation, dissolution data obtained in buffered solutions were omitted from our comparisons.

Perhaps the most noteworthy feature in the $k_d^*$ data shown in Figs. 5 and 6 are the *apparent* high dissolution rates at 25°C. We do not believe this behavior is due to fines dissolution, since our sample preparation was very effective in removing fines as verified by SEM observations given in Fig. 4c and d. Apparent high dissolution rates were observed in our experiments with the *Batch Bottle* and *Packed Bed* reactor systems with Ottawa sand as well as by Brady and Walther (1990) who used crushed quartz crystals from Hot Springs, Arkansas. Because dissolution rates are intrinsically very slow at 25°C, surface rearrangements or chemical annealing takes a much longer time than required at higher temperatures. For example, with an activation energy of about 97 kJ/mol, the intrinsic dissolution rate increases 20-fold for a 25°C increase in temperature from 25° to 50°C. Long-term *Batch Bottle* experiments conducted for up to 550 days (18 months) indicate a continual approach to the least-squares regression lines in Figs. 5 and 6. We believe this is due to a gradual annealing process that eventually results in a steady-state surface structure for dissolving quartz.

There are two sets of *Batch Bottle* experiment results plotted in Figures 5 and 6. The first set was performed on Ottawa sand using the standard sample preparation procedures plus an additional soaking in 70°C water for 10 days. Data from this set has the higher dissolution rate constant. The second set of experiments was performed on Ottawa sand taken from the *Spinning Basket* reactor after exposure to temperatures from 70°-150°C for a period of 50 days. This batch of sand should have annealed somewhat with a very low concentration of "high energy" sites remaining. The second data set reached steady state in six months and agrees well with the correlation in Figs. 5 and 6. The first set of experiments have been reacting for 18 months and are still not at steady-state. Nevertheless, we plotted the values in Figs. 5 and 6 for comparison. We anticipate that if we wait long enough, the first set of *Batch Bottle* experiments will agree with the correlations presented in Figures 5 and 6. We could estimate the time required to reach steady-state at 25°C based on our experiments at higher temperatures, but this extrapolation would be inaccurate since the activation energy for removal of the "high energy" sites will be less than for steady-state quartz dissolution.

Clearly more work needs to be done to quantitatively characterize how the surface morphology of quartz on a molecular-level influences these kinetic phenomena. Given the inherently complex nature of quartz hydrolysis and dissolution, the simplicity of the global correlation given by Eqn. (2) is even more striking.

## CONCLUSIONS

A general empirical correlation for estimating the intrinsic dissolution rate of quartz in pure water from 25° to 625°C was presented. Data obtained from five different apparatus in this study correlated favorably to rate measurements reported by seven other research groups using both nominal and BET-determined surface area bases. More than eleven orders of magnitude of variation of dissolution rate occur over a 600°C temperature change exhibiting Arrhenius-like behavior with a global activation energy of about 97 kJ/mol $SiO_2$. Discrepancies in low temperature (25°C) measurements were resolved by waiting sufficiently long to permit annealing processes to produce a "steady-state" dissolving surface.

***Acknowledgements.*** The authors would like to thank our colleagues at Los Alamos National Laboratory who assisted us in carrying out this work. In particular, C. Holley, R.M. Potter, D. Counce, P. Trujillo, the late L. Blatz, R. Charles, M.C. Smith, R.B. Duffield, D. Duchane, J. Albright, J.E. Mock, H. Murphy and A.W. Laughlin provided stimulating discussion, analytical support and critiques of our work over the past 15 years. The U.S. Department of Energy, Geothermal Technology Division, through the hot dry rock geothermal energy project also provided financial support for a portion of the work discussed in this paper. We also gratefully acknowledge the support provided by Alice Colby in preparing the manuscript for publication.

## REFERENCES


ANDERSON, G.M. and BURNHAM, C.W. (1965) The solubility of quartz in supercritical water. *Amer. J. Sci.* **263**, 494-511.

ARMSTEAD, H.C.H. and TESTER, J.W. (1987) Heat mining. *E&F N. Spon, London,* Section 10.4.

BRADY, P.V. and WALTHER, J.V. (1990) Kinetics of quartz dissolution at low temperatures. *Chem. Geol.* **82**, 253-264.

CASEY, W.H., LASAGA, A.C., and GIBBS, G.V. (1990) Mechanisms of silica dissolution as inferred from the kinetic isotope effect. *Geochim. Cosmochim. Acta* **54**, 3369-3378.

CHARLES, R.W., HOLLEY, C.E., TESTER, J.W., GRIGSBY, C.O., and BLATZ, L.A. (1979) Experimentally determined rock-fluid interactions applicable to a natural hot dry rock geothermal system. *TMS Paper Selection Report A80-8, The Metallurgical Society of AIME, Warrendale, PA.*

CRERAR, D.A. and ANDERSON, G.M. (1971) Solubility and solvation reactions of quartz in dilute hydrothermal solutions. *Chem. Geol.* **8**, 107-122.

DOVE, P.M. and CRERAR, D.A. (1990) Kinetics of quartz dissolution in electrolyte solutions using a hydrothermal mixed flow reactor. *Geochim. Cosmochim. Acta* **54**, 955-969.

FOURNIER, R.O. and ROWE, J.J. (1966) Estimation of underground temperature from the silica content of water from hot springs and wet-steam wells. *Amer. J. Sci.* **264**, 685-697.

FOURNIER, R.O. and POTTER, R.W. II (1982) An equation correlating the solubility of quartz in water from 25° to 900°C at pressures up to 10,000 bars. *Geochim. Cosmochim. Acta* **46**, 1969-1973.

GALLAGHER, J.S. and HAAR, L. (1985) Steam tables -- NBS standard reference database 10. *U.S. National Institute of Standards and Technology, Thermophysics Division*, Gaithersburg, MD.

GRIGSBY, C.O. (1989) Kinetics of rock-water reactions. *Ph.D. Thesis, Chemical Engineering Department, Massachusetts Institute of Technology*, Cambridge, MA.

GRIGSBY, C.O., TESTER, J.W., TRUJILLO, P.E. and COUNCE, D.A. (1989) Rock-water interactions in the Fenton Hill, New Mexico hot dry rock geothermal system. 1. Fluid mixing and chemical geothermometry. *Geothermics* **18** (5/6), 629-656.

GRIGSBY, C.O., and TESTER, J.W. (1989) Rock-water interactions in the Fenton Hill, New Mexico hot dry rock geothermal system. 2. Modeling geothermal behavior. *Geothermics* **18** (5/6), 657-676.

HEMLEY, J.J., MONTOYA, M., MARINENKO, J.W. and LUCE, R.W. (1980) Equilibria in the system $Al_2O_3$-$SiO_2$-$H_2O$ and some general implications for alteration/mineralization processes. *Econ. Geol.* **75**, 210-228.

ILER, R.K. (1955) *The Colloid Chemistry of Silica and the Silicates.* Cornell University Press.

ILER, R.K. (1979) *The Chemistry of Silica..* John Wiley and Sons.

KENNEDY, G.C. (1950) A portion of the system silica-water. *Econ. Geol.* **45**, 629-653.

KITAHARA, S. (1960) The solubility equilibrium and the rate of solution of quartz in water at high temperatures and high pressures. *Rev. Phys. Chem. Japan* **30** (2), 122-130.

MOREY, G.W. and HESSELGESSER, J.M. (1951) The solubility of quartz and some other substances in superheated steam at high pressures. *Amer. Soc. Mech. Eng. Trans.* **73**, 865-872.

O'CONNOR, T.L. and GREENBERG, S.A. (1958) The kinetics for the solution of silica in aqueous solutions. *J. Phys. Chem.* **62** (10), 1195-1198.

RICHARDS, H.G., SAVAGE, D. and ANDREWS, J.N. (1992) Granite-water reactions in an experimental hot dry rock geothermal reservoir, Resernanowes test site, Cornwall, U.K. *Applied Geochem.* **7**, 193-222.

RIMSTIDT, J.D. and BARNES, H.L. (1980) The kinetics of silica-water reactions. *Geochim. Cosmochim. Acta* **44**, 1683-1699.

ROBINSON, B.A. (1982) Quartz dissolution and silica deposition in hot dry rock geothermal systems. *M.S. Thesis, Chemical Engineering Department, Massachusetts Institute of Technology*, Cambridge, MA.

ROBINSON, B.A., TESTER, J.W. and BROWN, L.F. (1988) Reservoir sizing using inert and chemically reacting tracers. *SPE Formation Evaluation* **2**, 227-234.

SIEBERT, H., YOUDELIS, W.V., LEJA, J. and LILGE, E.O. (1963) The kinetics of the dissolution of crystalline quartz in water at high temperatures and high pressures. *Unit Processes in Hydrometallurgy, The Metallurgical Society of AIME Conference* **24**, 284-299.

SIEVER, R. (1962) Silica solubility 0°-200°C and the diagenesis of siliceous sediments. *J. Geol.* **70**, 127-150.

TESTER, J.W., HOLLEY, C.E. and BLATZ, L.A. (1977) Solution chemistry and scaling in hot dry rock geothermal systems. *83rd National Meeting of the American Institute of Chemical Engineers*, Houston.

VAN LIER, J.A., DE BRUYN, P.L. and OVERBEEK, J.Th.G. (1960) The solubility of quartz. *J. Phys. Chem.* **64**, 1675-1682.

WEILL, D.F. and FYFE, W.S. (1964) The solubility of quartz in $H_2O$ in the range 1000-4000 bars and 400-550°C. *Geochim. Cosmochim Acta* **28**, 1243-1255.

WHITE, A.F. and PETERSON, M.L. (1990) The role of reactive-surface-area characterization in geochemical kinetic models. In *Chemical Modeling of Aqueous Systems II (Chapter 35)*, (eds. D.C. Melchior and R.L. Bassett) *ACS Symposium Series 416*, Washington, D.C., 461-475.

WHITE, A.F. and PETERSON, M.L. (1990) The role of reactive surface areas in chemical weathering. *2nd Inter. Symp. Geochemistry of Earth's Surfaces and of Mineral Formation, July 2-8, 1990, Aixen Provences, France*, 334-336.